EARTH SURFACE PROCESSES AND LANDFORMS
Earth Surf. Process. Landforms **40**, 1254–1269 (2015)

Published online 17 March 2015 in Wiley Online Library
(wileyonlinelibrary.com) DOI: 10.1002/esp.3718

Evidence for climatic and hillslope-aspect controls on vadose zone hydrology and implications for saprolite weathering

Abigail L. Langston,[1]* Gregory E. Tucker,[1] Robert S. Anderson[2] and Suzanne P. Anderson[3]
[1] Cooperative Institute for Research in Environmental Sciences (CIRES) and Department of Geological Sciences, University of Colorado, Boulder, CO 80309, USA
[2] Institute of Arctic and Alpine Research (INSTAAR) and Department of Geological Sciences, University of Colorado, Boulder, CO 80309, USA
[3] Institute of Arctic and Alpine Research (INSTAAR) and Department of Geography, Boulder, CO 80309, USA

Received 4 July 2014; Revised 16 January 2015; Accepted 28 January 2015

*Correspondence to: Abigail L. Langston, Department of Geological Sciences, University of Colorado, Boulder, CO 80309. E-mail: abigail.langston@colorado.edu

ESPL
Earth Surface Processes and Landforms

ABSTRACT: Through the delivery of water in snowmelt, climate should govern the rate and extent of saprolite formation in snow-dominated mountain watersheds, yet the mechanisms by which water flows deeply into regolith are largely unexplored. In this study we link rainfall, snow depth, and water content data from both soil and shallow saprolite to document vadose zone dynamics in two montane catchments over 2 years. Measurements of snow pack thickness and soil moisture reveal strong contrasts between north- and south-facing slopes in both the timing of meltwater delivery and the duration of significant soil wetting in the shallow vadose zone. Despite similar magnitudes of snowmelt recharge, north-facing slopes have higher sustained soil moisture compared to south-facing slopes. To help interpret these observations, we use a 2D numerical model of vadose zone dynamics to calculate the expected space–time moisture patterns on an idealized hillslope under two wetting scenarios: a single sustained recharge pulse versus a set of short pulses. The model predicts that the duration of the recharge event exerts a stronger control on the depth and residence time of water in the upper unsaturated zone than the magnitude of the recharge event. Model calculations also imply that water should move more slowly through the subsurface and downward water flux should be substantially reduced when water is applied in several pulses rather than in one sustained event. The results suggest that thicker soil and more deeply weathered rock on north-facing slopes may reflect greater water supply to the deep subsurface. Copyright © 2015 John Wiley & Sons, Ltd.

KEYWORDS: soil moisture; vadose zone; weathering

Introduction

Understanding the processes that transform bedrock into saprolite is fundamental to understanding sediment production on hillslopes, soil development, and watershed biogeochemical cycles. The weathering of fresh bedrock to saprolite – *in situ* rock that has been chemically altered and mechanically weakened by chemical weathering to the point that it can be augered by hand – sets the stage for the production of mobile regolith and its subsequent transport downslope (Anderson *et al.*, 2007). The degree and rate of weathering in the saprolite play important roles in the chemical weathering fluxes in a landscape and the rate that mobile regolith is transported downslope (Dixon *et al.*, 2009). It has long been known that the transformation of parent rock into a developed soil depends on a complex interaction of lithological, topographical, climatic, and biological factors (Jenny, 1941). More recently, studies have recognized that the production rate and spatial distribution of saprolite, a transitional material between rock and soil, depend on a complex interaction of climatic, lithological, erosional, and tectonic factors (summarized by Brantley and Lebedeva, 2011). The chemical reactions that produce saprolite are mediated by water; therefore the flux of moisture to the weathering zone should exert a first-order control on the rate of saprolite evolution. Where there is ample supply of fresh parent material, locations with warm, wet climates experience higher rates of chemical weathering than cold or dry climates (White and Blum, 1995; White *et al.*, 1998; Riebe *et al.*, 2004). Recent studies on chemical weathering in soil and saprolite on hillslopes found a correlation between climate, especially precipitation, and chemical weathering rates in systems where the chemical weathering rate is limited by the mineral reaction kinetics (Dixon *et al.*, 2009; Rasmussen *et al.*, 2011; Ferrier *et al.*, 2012). Models of bedrock weathering often assume a steady and uniform downward flux of water. One implication of these models is that, all else being equal, the potential for chemical alteration is greatest near the surface, where infiltrating water is furthest from chemical saturation. As water moves

progressively deeper in the profile, it approaches chemical saturation and the weathering rate approaches zero (Brantley and White, 2009).

In semi-arid regions, however, water movement through the shallow subsurface is more complex than the simple picture of a steady, uniform downward flux suggests. If the near surface soil is relatively dry, the water input from a rainstorm or snowmelt event may be trapped in the upper few centimeters of the soil profile, and subsequently released back to the atmosphere through evapotranspiration. Consequently, the overall flow of water through the near-surface may be substantially greater than in deeper areas of the unsaturated zone. Moreover, the extent to which water can penetrate below the upper few tens of centimeters may depend on both the magnitude and the relative timing of rain or snowmelt events. One might hypothesize, for example, that brief pulses of water infiltration are less likely to penetrate deeply than a single, sustained pulse, which could produce higher near-surface moisture and create a higher effective hydraulic conductivity.

These complexities associated with water input raise interesting questions regarding the role of shallow subsurface hydrology in weathering patterns on hillslopes. What are the frequency and magnitude characteristics of water delivery to the soil–saprolite interface? How do water fluxes and peak moisture vary with depth? To what extent are space–time patterns of water delivery influenced by the timing of rainfall and snowmelt? Can timing be significantly influenced by slope aspect? And is there a correlation between aspect, weathering extent, and water input timing? Here, we seek to build a foundation for addressing these questions by (i) collecting and analyzing data on snow depth, soil moisture, and shallow saprolite moisture in two semi-arid catchments in the Colorado Front Range, and (ii) using a two-dimensional model of vadose zone dynamics to explore the influence of water input timing on space–time moisture patterns in the upper few meters of soil and saprolite.

Background

Several studies have used numerical modeling to explore the chemical evolution of bedrock to saprolite and mobile regolith (summarized by Brantley and White, 2009), and some modeling studies are beginning to acknowledge the direct role that hydrological processes play in chemical weathering (Lebedeva *et al.*, 2007, 2010; Maher, 2010). Maher (2010) recognized that chemical weathering rates are strongly dependent on the residence time and flow rate of water in the subsurface, with faster chemical weathering rates associated with faster fluid flow rates. Lebedeva *et al.* (2010) developed a model that included an erosion component and considered both advective and diffusive solute transport for moving the chemical weathering front. They found that small changes in either fluid velocity or erosion rate can significantly impact the thickness of the weathering zone. One of the important underlying assumptions in the analyses of Lebedeva *et al.* (2010) is that the weathering zone experiences a spatially uniform downward flux of water. While this is a reasonable simplification in some landscapes, or for the exploration of model sensitivity, studies of vadose zone dynamics reveal a more complicated picture.

Slope angle, soil depth, and bedrock permeability all play a role in determining lateral and vertical flow paths in the hillslope subsurface (Hopp and McDonnell, 2009). Antecedent soil moisture also exerts an important influence on the subsurface flow paths in hillslopes; only following the largest storm events do antecedent conditions cease to exert a strong control on subsurface flow paths (Woods and Rowe, 1996). The questions of how much recharge infiltrates into the bedrock, how this deep seepage component scales from hillslope to catchment scale, and what role deep seepage plays in the hydrological function of hillslopes are being addressed (Graham *et al.*, 2010), but integrating hillslope hydrology and chemical weathering remains a frontier that is largely unexplored.

Numerous studies have recognized that fractures in bedrock can play a major role in both water transport and the weathering by water beneath hillslopes in small, steep catchments (e.g. Montgomery *et al.*, 1997; Anderson *et al.*, 1997; Kosugi *et al.*, 2006; Ebel *et al.*, 2007). Infiltrating storm water or snowmelt that flows through the vadose zone weathers bedrock en route to the water table (Anderson *et al.*, 2002). Hillslope aspect can exert strong control on weathering rates in soils (Egli *et al.*, 2006), on snow depth and soil moisture (Williams *et al.*, 2008), and on ground temperatures (Anderson *et al.*, 2013). In the Northern Hemisphere, north-facing hillslopes tend to be colder and their snow packs more persistent, whereas south-facing hillslopes tend to be warmer and have shorter-lived snow packs.

To explore the impact of aspect and climate on the delivery of water into the soil and uppermost saprolite and potential chemical weathering in the saprolite and deeper subsurface, we use measurements of rainfall, snow depth, and water content in soil and uppermost saprolite to inform a numerical model of unsaturated flow in a two-dimensional idealized hillslope. Characterizing differences in hydrology is a crucial first step for understanding differences in the development of the weathering front. In addition to matrix flow through the soil and upper saprolite, the model also includes fractures in the saprolite, which are potentially important avenues for routing water deep in the subsurface (Beven and Germann, 2013). The goal of this theoretical analysis is to explore how the duration of recharge, independent of the magnitude of recharge, affects water fluxes and subsurface flow paths through the saprolite.

Field Site

The influence of variations in climate on subsurface flow paths and saprolite formation is studied in the Boulder Creek watershed, located in Front Range of Colorado (Figure 1a). The Boulder Creek watershed ranges in elevation from 1480 to 4120 m and bedrock includes Precambrian Boulder Creek granodiorite and metamorphic sillimanite gneiss. The mean annual precipitation and percent precipitation that falls as snow increase with elevation, while mean annual temperature decreases with elevation (Cowie, 2010). We present rainfall, snow depth, and water content data from 2010 and 2011 that were collected in two small catchments within the Boulder Creek watershed. The Betasso catchment (Figure 1b), located at 1900 m above sea level, receives 47 cm precipitation per year and has a mean annual air temperature of 10°C (Cowie, 2010). This catchment is representative of a dry foothills montane ecosystem and is largely vegetated by ponderosa pine trees (*Pinus ponderosa*). Gordon Gulch (Figure 1c), located at 2600 m above sea level, is an east–west trending catchment with mean annual precipitation of 55 cm and mean annual air temperature of 6°C (Cowie, 2010).

The north- and south-facing hillslopes of Gordon Gulch offer an opportunity to explore the effects of slope aspect on the hydrology and geomorphology of the catchment. The hillslopes at Gordon Gulch are convex upward in profile and have a relatively thin mantle of soil (15–100 cm) overlying saprolite. The north-facing slope is densely forested by lodgepole pine trees (*Pinus contorta*) and retains a seasonal snow pack from late fall to mid spring. The south-facing

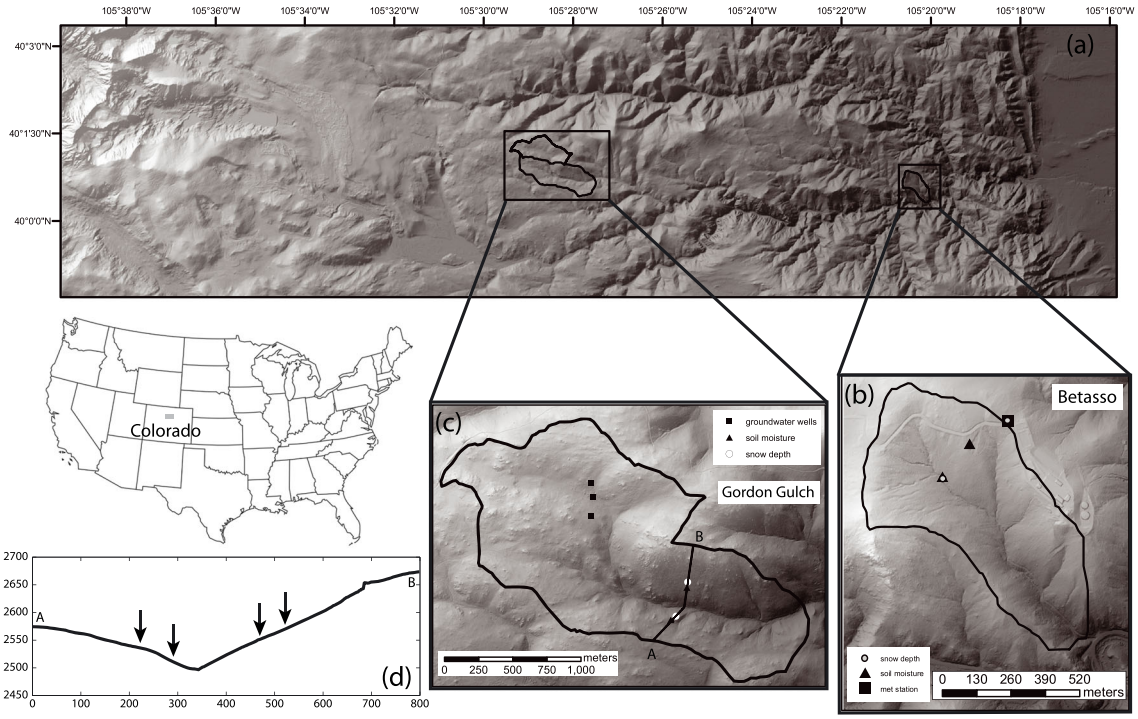

Figure 1. (a) Shaded relief map at 10 m resolution showing Boulder Creek catchment from the Continental Divide (4000 m) to the High Plains (1600 m). The inset maps show the two instrumented sub-catchments. (b) Betasso catchment and (c) Gordon Gulch. Instrument locations in each sub-catchment are shown. (d) Cross-section of Gordon Gulch with sensor locations on each slope indicated by arrows.

slope is vegetated by grasses, shrubs, and sparsely distributed ponderosa pine trees, similar to the Betasso catchment. The south-facing slope is generally free of snow during the winter, except for a few days immediately following snow events. The depth to the weathered bedrock and the thickness of saprolite is greater on the north-facing slope of Gordon Gulch than on the south-facing slope. Soil is also thicker on the north-facing slope and the underlying saprolite appears more intensely weathered (Anderson *et al.*, 2011). Experiments to determine the tensile strength of rock cores recovered from 1–2 m depth on the north- and south-facing slopes show that rock is weaker and presumably more weathered on the north-facing slope than on the south-facing slope (Kelly, 2012). Shallow seismic refraction surveys in Gordon Gulch reveal that low velocities associated with saprolite extend to approximately 8 m depth on the north-facing slope, compared to about 4 m depth on the south-facing slope (Befus *et al.*, 2011).

Drilling logs from groundwater wells drilled at Gordon Gulch (Figure 1c) offer a glimpse into the deep subsurface on the north- and south-facing slopes. These corroborate the shallow geophysical survey results, suggesting that the interface between saprolite and fresh bedrock is deeper on the north-facing slope. On the north-facing slope, the depth to the saprolite-fresh bedrock boundary is ∼14.6 m, whereas on the south-facing slope the depth to this interface is ∼7.4 m. Depth to groundwater during the study period ranges from 8.5 to 9.5 m on the north-facing slope and from 3 to 6.5 m on the south-facing slope. Drilling notes also indicate that drilling in the bedrock on the south-facing slope was slow compared to the north-facing slope, suggesting that rock on the south-facing slope is less weathered.

Data Collection and Analysis

Precipitation and water content data from the north- and south-facing slopes of Gordon Gulch and the lower-elevation Betasso catchment allow us to explore climatic controls on hillslope hydrology. We analyze rainfall, snow depth, soil moisture, and matric potential measurements in these two catchments that were collected over a period of 2 years to quantify the magnitude and timing of water delivery to the subsurface.

Instrumentation

In order to determine how hillslope aspect affects soil moisture dynamics, soil moisture sensors were placed in a 300 m long transect that spanned the north- and south-facing hillslopes at Gordon Gulch (Figure 1d). Twenty-four soil moisture sensors (Campbell Scientific CS616) were placed in 12 locations at 5 cm below the surface and ∼25 cm below the surface (Hinckley *et al.*, 2014) (Figure 2a). Soil moisture was measured every 10 min. Snow depth, which can change significantly within hours in this sub-alpine catchment, was measured using 16 Judd sonic snow depth sensors that were placed in four locations along the same north–south trending transect. The sensors recorded snow depth with an accuracy of ±1 cm every 10 min.

Soil moisture sensors (Decagon EC-5) and matric potential sensors (Decagon MPS-1) were installed in the Betasso catchment (Figure 2b). Three sets of paired sensors were installed in vertical soil–saprolite profiles at two locations (the Gully site and the Borrow Pit site), ranging in depth from 15 to 110 cm. Four of the six sensor pairs at Betasso were installed in saprolite at depths ranging from 40 to 110 cm. Snow depth was determined using five Judd sonic snow depth sensors located in the Betasso catchment. Snow depth was measured with an accuracy of ±1 cm every 10 min. Rainfall was measured and recorded every 10 min with a tipping bucket rain gage located on a ridge about 140 and 330 m, respectively, from the two sensor sites.

Figure 2. Photographs of representative sensor sites at Gordon Gulch and Betasso. (a) South-facing slope of Gordon Gulch prior to sensor installation. Arrows mark approximate location of sensors. Total depth of the pit is 25 cm. (b) Gully Site at Betasso with soil moisture and matric potential sensor pairs shown. Total depth of the pit is 80 cm. This figure is available in colour online at wileyonlinelibrary.com/journal/espl

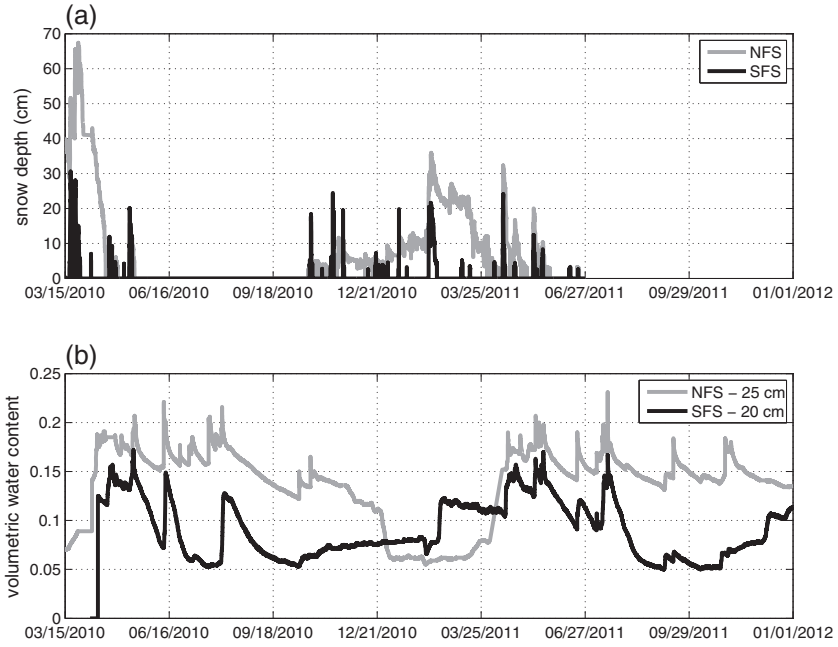

Figure 3. Snow depth and soil moisture measurements from representative sensors on the north- and south-facing slopes of Gordon Gulch. (a) Continuous snow depth measurements show the snow pack on the north-facing slope that lasts from late fall to early spring and maximum snow depth of 68 cm. Most events on the south-facing slope are smaller and remain on the ground for shorter durations. (b) Soil moisture measurements at 25 cm depth (sensor GGL-NF-SP4-R4-CS616-25) show that on the north-facing slope soil moisture increased following spring snowmelt and remained elevated through much of the summer and fall. On the south-facing slope, soil moisture (sensor GGL-SF-SP9-R2-CS616-25) increased following discrete snowmelt events and declined rapidly during the summer and fall.

Snow depth and soil moisture observations

Gordon Gulch

To characterize how temporal variability of shallow soil moisture is influenced by snow melt in Gordon Gulch, we analyze soil moisture and snow depth data from 2 years of monitoring records. Snow depth and duration of snow cover are strongly controlled by hillslope aspect. During the 2009–2010 winter, the north-facing slope had a seasonal snow pack that reached a maximum depth of 70 cm in March 2010 (Figure 3a). During the 2010–2011 winter, the north-facing slope was covered in snow from late October 2010 to late April 2011 and reached a maximum snow depth of 35 cm in February. The north-facing slope snow depth sensors measured a snow pack depth of 5–10 cm from late 2010 to early 2011, which is consistent with weekly manual snow depth measurements. Late spring snow events up to 30 cm deep occurred in May of both 2010 and 2011. The south-facing slope received the same amount of snowfall as the north-facing slope, but snow cover generally did not persist more than several days due to higher solar radiation relative to the north-facing slope (Figure 3a). Maximum snow depth on the south-facing slope during the study period

reached ∼30 cm in February 2011 and the longest duration of snow cover on the south-facing slope was 8 days during early 2011.

Soil moisture in Gordon Gulch tends to remain elevated for longer periods on the north-facing slope. Soil moisture tends to be more dynamic on the south-facing slope, with rapid increases in moisture followed by relatively rapid decreases (Figure 3b). Soil moisture on the north-facing slope experienced a rapid increase in response to melting snow packs in April 2010 and 2011 (Figure 3b). Soil moisture on the north-facing slope remained elevated during the early summer in response to rain events, but began to decline during early fall 2010, reaching its lowest values during the winter of 2010–2011. Soil moisture on the south-facing slope was generally lower than on the north-facing slope, except during the winter. As on the north-facing slope, soil moisture on the south-facing slope increased in response to early spring snow melt, but values dropped much more quickly than on the north-facing slope (Figure 3b). By May of 2010, soil moisture on the south-facing slope was generally low (∼ 5 – 10%), but responded quickly to summer rain events. In February 2011, soil moisture increased sharply in response to the largest single snowmelt event of the study period on the south-facing slope. Soil moisture on the south-facing slope remained elevated during the spring, increased in response to two late spring snow events, and began to decrease during the summer months, reaching very low levels (∼ 5%) by late summer 2011.

Betasso catchment

During the study period (July 2010–January 2012), 60 cm of precipitation fell as rain at the Betasso catchment and 55 cm of precipitation fell as snow (Figure 4a). The shallowest sensors in the Betasso catchment showed the most variability in water content and matric potential in response to precipitation events (Figure 4). Here, we refer to matric potential in terms of the absolute value of pressure, so that a large negative pressure is called a high potential and a small negative pressure is a low potential. Water content increased at the upper sensor following a snow event in February 2011. Matric potential at the upper sensor simultaneously decreased dramatically, indicating a decrease in water tension. Following this snowmelt event, water content in the upper sensor declined rapidly, but matric potential remained low and increased much more slowly. A rain and snow event in April 2011 caused water content to increase sharply at all of the sensors, but to a smaller magnitude at the lowest sensor. Matric potential fell to the same level at all of the sensors, ∼10 kPa, following this rain and snow event. Over the next 30 days, water content declined rapidly at the upper sensor and remained steady at the middle and lowest sensors, while matric potential remained steady or increased slightly at the lowest sensor. A rain event in early May 2010 caused water content at the upper and middle sensors to increase sharply, but the lower sensor showed no response.

Two weeks following this precipitation in early May, a rain event in late May caused water content in the upper and middle sensors to increase further and caused water content in the lower sensor to increase to the highest recorded value

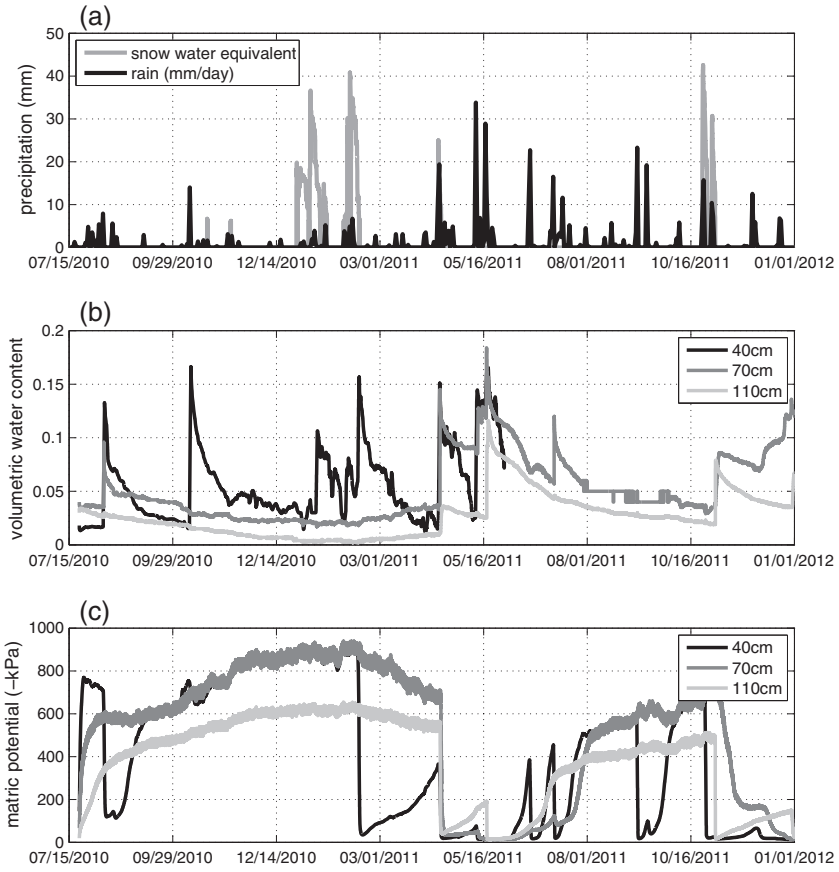

Figure 4. Precipitation, saprolite moisture, and matric potential measurements from the Betasso catchment. (a) Daily averages of rain and snow depth measurements. Snow depth measurements were converted to SWE using a snow density of 333 kg m^{-3}. (b) Water content measurements from the profile at the Borrow Pit. All of the sensors in this profile were installed in the saprolite, not the overlying soil. As the sensor at 40 cm depth malfunctioned in July 2011, data are unavailable after this date. (c) Absolute value of matric potential measurements from the Borrow Pit profile. Matric potential sensors are paired with water content sensors at 40, 70, and 110 cm below the surface.

during the study period. Matric potential remained very low through these events. Over a period of 10 days following the rain events in May 2011, water content declined and matric potential increased rapidly in the upper sensor and changed more slowly in the middle and lower sensors. A rain event in June 2011 caused rapid changes in water content and matric potential at the upper sensor, followed by rapid decay over 7 days. By July 2011, water content had decreased and matric potential had increased significantly at the upper sensor. Water content data are unavailable after July 2011, when the upper sensor malfunctioned.

Summary of snow depth and soil moisture observations

Measurements of snow pack thickness and soil moisture in Gordon Gulch reveal strong contrasts between the north- and south-facing slopes. The snow pack on the north-facing slope accumulates all winter, then melts in one spring event, producing a deep, long-duration wetting event in the subsurface. The south-facing slope is intermittently covered by snow, which melts in the days following the event. As a result of these small, frequent melt events, soil moisture on the south-facing slope is more variable with time. Soil moisture and matric potential observations at Betasso show that longer periods of recharge are necessary to sufficiently wet the upper part of the profile and drive water deep into the subsurface. These results motivate modeling efforts in which we attempt to understand how differences in snowmelt timing influence the quantity and depth distribution of moisture in the soil and upper saprolite.

Modeling Unsaturated Zone Flow

The aspect-related differences in snow cover, shallow soil moisture, and water content response in saprolite are used to guide two-dimensional unsaturated zone flow models on an idealized hillslope. These models inform us on the conditions necessary to route water deep into the saprolite through both its matrix and its fractures. The complex architecture of the unsaturated zone necessitates a model capable of capturing variable permeability to represent the different hydrological properties in the soil, saprolite, and fractures. The two-dimensional distribution of water content in partially saturated porous media, is described by the Richards equation:

$$\frac{\partial\theta}{\partial t} = \frac{\partial\left[K(\theta)\left(\frac{\partial\psi}{\partial x}\right)\right]}{\partial x} + \frac{\partial\left[K(\theta)\left(\frac{\partial\psi}{\partial z}+1\right)\right]}{\partial z} \quad (1)$$

where θ is volumetric water content (VWC), K is hydraulic conductivity [L/T], ψ is the capillary pressure head [L], x is the horizontal direction [L], and z is depth below the soil surface [L]. Computing two-dimensional flow dynamics in a medium with spatially and temporally varying K, θ, and ψ requires a numerical solution. Here we used VS2DI (version 1.3), a program developed by the USGS for modeling flow in the unsaturated zone (Healy, 2008). VS2DI uses a finite-difference method to solve the Richards equation for flow in a variably saturated medium. VS2DI uses the van Genuchten equations (van Genuchten, 1980) to describe the nonlinear relationship between pressure head and moisture content and hydraulic conductivity. The relation between water content and pressure head is given by

$$\theta(\psi) = \theta_r + \frac{\theta_s - \theta_r}{[1 + (\alpha|\psi|)^n]^{1-1/n}} \quad (2)$$

where $\theta(\psi)$ is soil water content as a function of capillary pressure head, θ_r is residual soil water content, θ_s is saturated soil water content, and α and n are parameters related to air entry suction and pore size distribution, respectively. The relation between conductivity and pressure head is given by

$$K(\psi) = \frac{\left[1 - (\alpha\psi)^{n-1}\left(1 + (\alpha\psi)^n\right)^{-m}\right]^2}{[1 + (\alpha\psi)^n]^{m/2}}, \quad m = 1 - 1/n \quad (3)$$

where $K(\psi)$ is unsaturated hydraulic conductivity as a function of capillary pressure head.

Model setup

Our aim was to calculate the moisture dynamics that are characteristic of a setting like that of the Boulder Creek watershed, with convex upward hillslopes that receive most of their moisture from seasonal snowmelt. To that end, the models are set up as an idealized hillslope that represents the lowermost portion of the hillslopes at Gordon Gulch. The two-dimensional grid was 5.5 m high by 10 m long, with cell spacing of 4 cm. This spacing is fine enough to resolve the fractures and the soil–saprolite interface, while allowing reasonable computation time. The scaled-down model grid also allows us to evaluate flow dynamics near the stream as well as higher on the hillslopes within a geologically reasonable framework that includes an unsaturated zone that is several meters thick and local model hillslopes that span the range of slopes found in Gordon Gulch (Figure 1d). A model on the scale of the hillslopes at Gordon Gulch (~300 m in length) is not necessary to capture the unsaturated flow dynamics in the top several meters, where the flow direction is primarily vertical and lateral transport limited.

In the model, 70 cm of soil overlies several meters of saprolite, which is cut through by three vertical fractures (Figure 5). Because the spatial distribution and connectedness of fractures and the relative importance of fracture flow in the shallow, highly weathered saprolite and in the deep, unweathered bedrock in the hillslopes are not known, a simple continuum model approach was appropriate for this study rather than a discrete fracture model (Glass *et al.*, 1995; Berkowitz, 2002). Fractures in the model are simply meant to show how preferential flow paths can influence moisture distribution and

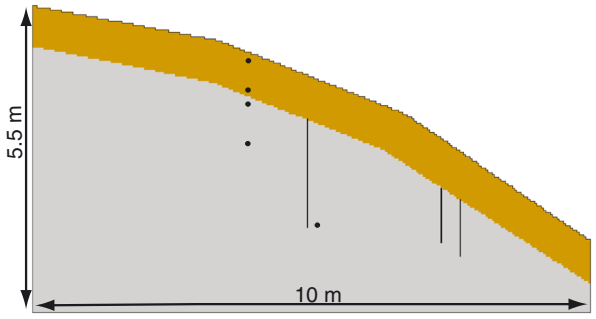

Figure 5. Schematic illustration of the unsaturated zone hillslope model. The left side of the model represents the hillcrest and the right side of the model intersects with a small perennial stream. The model domain is 5.5 m high and 10 m wide. 70 cm of soil overlies saprolite, which has three fractures (vertical black lines). Five markers indicate the positions of model cell output points at which the degree of saturation and volumetric water content were recorded at each time step of the model run. This figure is available in colour online at wileyonlinelibrary.com/journal/espl

Table I. Hydraulic properties of materials in unsaturated zone models

Material	K (m d^{-1})	ϕ	α (1 m^{-1})	n
Soil	7.6	0.55	5.35	1.31
Saprolite	0.02	0.2	0.75	7
Fracture	2	0.1	0.75	7

potential chemical weathering in a hillslope. Spacing between fractures in the model ranges from 3 to 0.3 m in order to capture the range of fracture spacing (<10 cm to 7 m) measured in outcrops at the Betasso catchment (Dengler, 2010). Each model fracture is represented by one column of cells 2 cm wide that extends several meters into the saprolite, starting at the soil–saprolite boundary. The fractures in the model have a porosity of 0.1, making their effective aperture 2 mm. The fractures are thus approximated as highly conductive porous media reflecting the likelihood that fractures in saprolite will have rough walls and possibly contain rock fragments.

The hydraulic properties of the soil and saprolite are determined from a combination of laboratory experiments, field data, and previously documented values (Table I). Soil cores taken from the four soil pits in Gordon Gulch where the soil moisture sensors were installed were analyzed for various hydraulic properties (Hinckley *et al.*, 2014). Saturated hydraulic conductivity, porosity, and van Genuchten parameters from the soil core analysis were used in the model to characterize the hydraulic properties of the soil layer.

As a detailed analysis of the hydraulic properties of the saprolite was not available, we make estimates for these values from field data and previously published values. Saprolite hydraulic conductivity is estimated from wetting front travel times between soil moisture sensors in saprolite at the Betasso catchment. Travel times of a pulse of water from two rain events between two sensors spaced 30 cm apart were 18.5 and 9.3 h, yielding estimated hydraulic conductivities of 0.39 to 0.77 m d^{-1}, respectively. This is comparable to previously published values of hydraulic conductivity in weathered granite in the Idaho batholith, which range from 0 to 1.7 m d^{-1} (Megahan and Clayton, 1986). Hydraulic conductivity measurements derived from falling-head tests on weathered granite cores from Japan range from 0.015 to 0.03 m d^{-1}, providing an estimate for matrix hydraulic conductivity (Katsura *et al.*, 2009). The saprolite matrix is assigned a saturated hydraulic conductivity on the lower end of the range of measured hydraulic conductivities in weathered granite (0.02 m d^{-1}), while the fractures are assigned a hydraulic conductivity at the higher end of the range (2 m d^{-1}) (Table I). The sensitivity of model results to the assigned hydraulic conductivity value is tested by decreasing K by one-half and increasing K by a factor of two and by a factor of four in additional model runs.

van Genuchten parameters for the saprolite were estimated by comparing the results of 110 model runs with moisture content data from sensors installed in saprolite at the Betasso catchment. These models were run using the assigned representative K value for saprolite (Megahan and Clayton, 1986; Katsura *et al.*, 2009) and spanned a large range of plausible α and n values. A 1-year model calculation was set up in VS2DI using recharge inputs from the Betasso meterological station for the year 2010. Model output points at which VWC was recorded were placed in the saprolite at the same depths as the soil moisture sensors in the Betasso Borrow Pit. VWC values at the three model output points in 110 model runs were compared with the VWC data from the sensors over 200 model days that included three precipitation events and a drying period of 100 days (Figure 6). The combination of α and n parameters that best matched the data was chosen for the saprolite van Genuchten parameters.

The fractures cutting through the saprolite are assigned the same α and n parameters as the saprolite, and the hydraulic conductivity of the fractures is two orders of magnitude larger and porosity was half of that in the saprolite. These values are chosen to capture the apparent increase in the hydraulic conductivity of saprolite with increasing scale due to preferential flow paths (Megahan and Clayton, 1986; Katsura *et al.*, 2009).

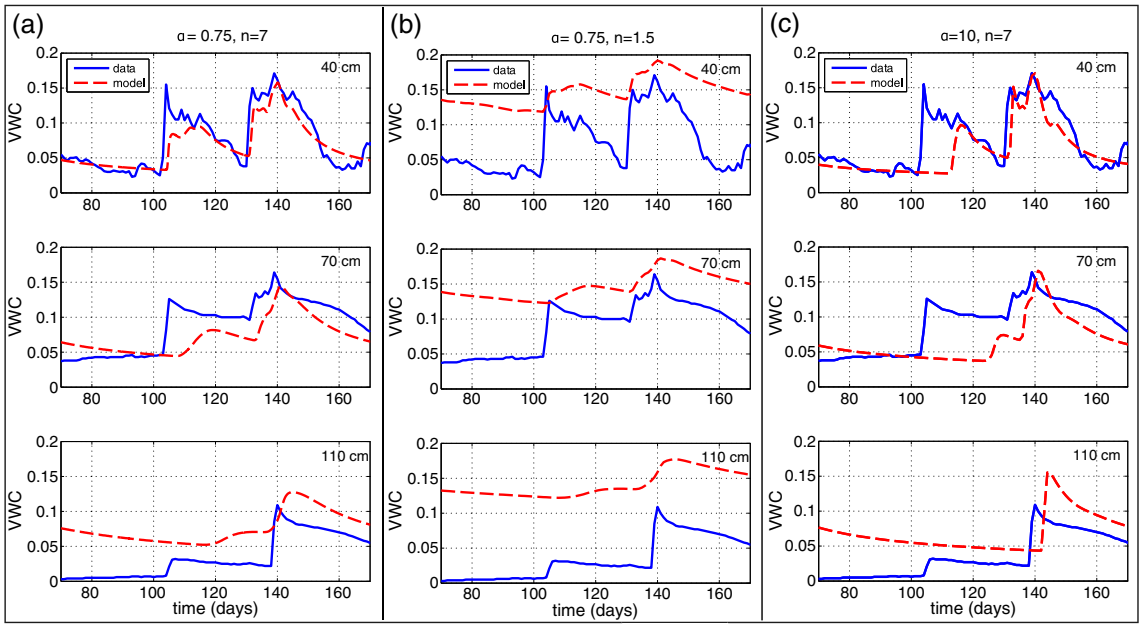

Figure 6. Model calibration of α and n parameters. VWC versus time from sensors at Betasso (solid lines) and model output (dashed lines). Results from model calibration runs for 40, 70, and 110 cm below the surface are shown. (a) Parameters used for model runs, $\alpha = 0.75$ and $n = 7$. (b) When $\alpha = 0.75$ and $n = 1.5$, model VWC decreases slower than VWC data from sensors. (c) When $\alpha = 10$ and $n = 7$ peaks in VWC are delayed compared to data from sensors. This figure is available in colour online at wileyonlinelibrary.com/journal/espl

A no-flux boundary condition is assigned to the upper hillslope side of the model. Seepage face boundaries are assigned to the bottom and lower hillslope side of the model. At seepage face boundary cells, total head is set to elevation head and fluxes are calculated. If the water fluxes are zero or directed out of the model, the simulation proceeds. If the calculated flux at a cell is directed into the model, the cell is set as a no-flux boundary (Lappala *et al.*, 1987). The horizontal seepage face produces a horizontal water table. Although a water table that subtly reflects the model topography would more accurately reflect conditions found in nature, the horizontal water table is suitable for our purposes because the depth from the model surface to the water table is similar to that found in Gordon Gulch. During periods of snowmelt, the top boundary condition is designated as a specified flux boundary, at which recharge is applied at a given rate. For intervals between snowmelt events, the top boundary is an evaporation boundary and the potential evaporation rate is set to 0.001 m d^{-1}. This relatively low value for potential evaporation rate is chosen to represent potential evaporation during the late winter and spring months, rather than a higher value of potential evaporation during the summer months (Western Regional Climate Center, 2012). In order to isolate the effect of the episodicity of recharge, the same potential evaporation rate was assigned to all model runs, despite differences in soil temperature and vegetation cover on the north- and south-facing hillslopes in Gordon Gulch. Because early spring snowmelt recharge precedes the onset of significant transpiration in this area (Sacks *et al.*, 2006), transpiration is not included in the model calculations. The sensitivity of model results to the assigned evaporation rate is tested by changing the evaporation rate by a factor of two in additional model runs. Prior to beginning the model runs that are analyzed in this study, all models were run until they reached periodic steady state by applying 29 cm of recharge over 24 days followed by 322 days of evaporation for two cycles.

Gordon Gulch models

The first set of models is driven by snow depth measurements from the north- and south-facing slopes in Gordon Gulch. The 2-year record of snow depth is converted into snow water equivalent by using the average late-spring density of the snow pack in Gordon Gulch. Measurements of snow density made in annual snow pit surveys at Gordon Gulch indicate that the average snow density between mid March and early May is 333 kg m^{-3}. Water is added to the model at the rate at which snow pack decreased. Six snowmelt events are applied to the north-facing slope model and 20 snowmelt events are applied to the south-facing slope over two model years. Over the 2-year model runs, the two hillslope models receive similar amounts of precipitation on the north- and south-facing slope models (59 and 54 cm, respectively), but the north-facing slope model experiences 515 days of evaporation, whereas the south-facing slope experiences 636 days of evaporation (Table II). Five model output points are placed in the model at various locations to record VWC and degree of saturation (Figure 5). The model output points are placed in the saprolite both to mimic field instrument setup and to understand the role played by fractures in routing water deep into the subsurface. Model output points are placed in the soil at 10 and 70 cm below the hillslope surface and in the saprolite at 90 and 145 cm below the ground surface and 15 cm away from the base of a fracture (Figure 5). In the Northern Hemisphere, north-facing slopes experience lower temperatures, less solar radiation, and are more likely to have a seasonal snow pack than south-facing slopes. Recognizing this, one can equate the terms used here, 'north-facing slope' and 'south-facing slope', with 'pole-facing slope' and 'Equator-facing slope' (respectively) so that the terms are applicable to hillslopes in the Southern Hemisphere.

Table II. Recharge and evaporation summary for model runs

Model run name	Total recharge (cm)	Number of recharge events	Days of evaporation
North-facing slope	59	6	515
South-facing slope	54	20	636
Concentrated recharge	58	2	644
Episodic recharge	58	12	644

Idealized models

We expect that the sunny south-facing slope would experience more evaporation in nature; the south-facing slope model experiences more days of evaporation because a seasonal snow pack is not present. To determine the extent to which subsurface flow paths depend on the timing of recharge, we also conduct a set of idealized modeling calculations that differ in neither the magnitude of input fluxes nor the number of days of evaporation. The model domain, parameters, and output points for these models were identical to the Gordon Gulch hillslope models; the model experiments differ from each other only in the timing of the application of 58 cm of recharge (approximately equal to the recharge applied to the north-facing slope model). A concentrated recharge model scenario is run for two more years with one large pulse of water per year, applied over 24 days, at a rate of 0.012 m d^{-1}, followed by 322 days of evaporation. An episodic recharge model scenario is run for 2 years in which repeated cycles of recharge and evaporation are modeled, with 4 days of recharge, added at 0.012 m d^{-1}, followed by 24 days of evaporation. After six recharge–evaporation periods, 202 days of evaporation followed (Table II).

Model analysis

Aspect control

To understand how the contrasting snowmelt patterns on north- and south-facing slopes influence flow dynamics and water input to the saprolite, we use VS2DI to calculate flow in the unsaturated zone in response to the estimated timing and magnitude of the observed melt events at Gordon Gulch. The models of the north- and south-facing hillslopes show distinct patterns in water content and flow paths through the hillslope (Figure 7).

After all of the recharge for one model year is added to both the north- and south-facing slope models, the soil is saturated to a similar degree. However, the wetting front penetrates ~3 m into the saprolite on the north-facing slope and only penetrates ~1 m into the saprolite on the south-facing slope (Figure 7a). Moisture content in the saprolite on the north-facing slope is higher than that on the south-facing slope after the last recharge was applied. Ten days following the last recharge, water starts to drain from the upper saprolite in both the north- and south-facing slope models and move through the hillslope (Figure 7b). Ten days after the last recharge, the wetting front reaches the water table in most places on the north-facing slope, whereas on the south-facing slope the wetting front is still ~1.5 m above the water table. In both models, the saprolite matrix near the fractures is drier than the rest of the saprolite, whereas the bases of the fractures are more saturated than saprolite at comparable depth. After 45 days of evaporation, the top several centimeters of soil and the ~0.5

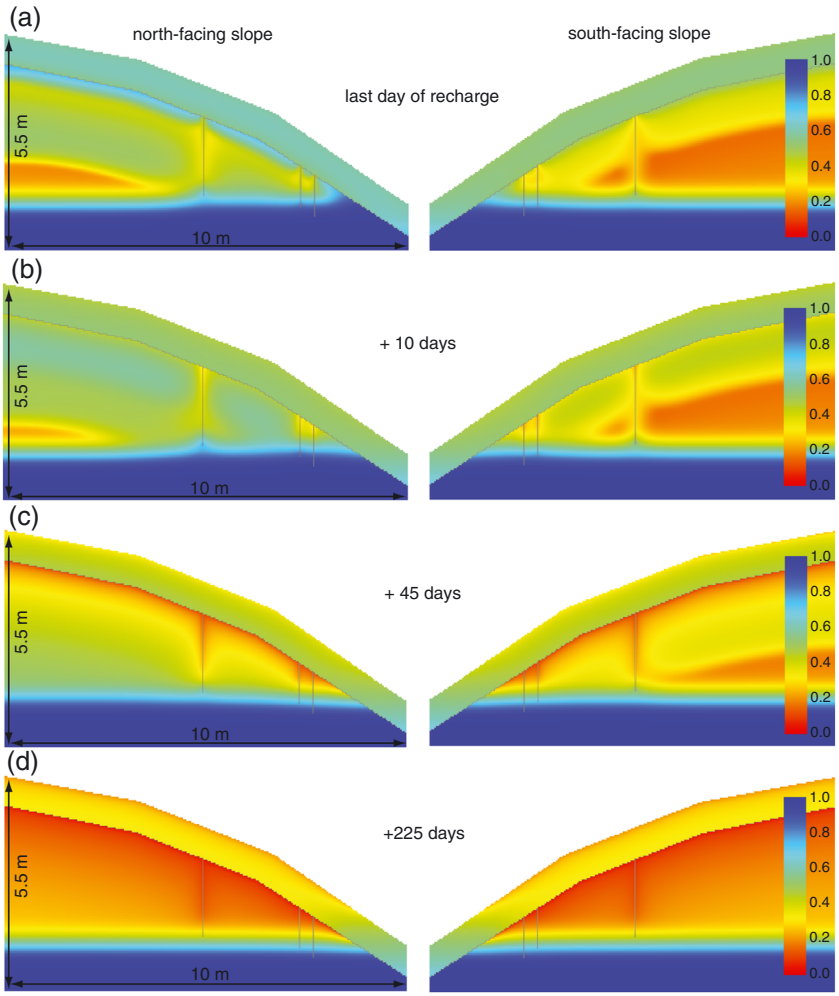

Figure 7. Degree of saturation of the entire model domain for the north- and south-facing slope model runs based on recharge input inferred from snow depth records at Gordon Gulch. The model domains are the same size (5.5 m high, 10 m wide). The three vertical lines in the model domain are fractures in the saprolite. The water table developed 1 m above the bottom boundary and did not fluctuate significantly during the entire model period. (a) Models on the last day of recharge in the first model year (model day 100) for both model runs. (b) Model domains 10 days after the last recharge event. (c) Model domains 45 days after the last recharge event. (d) Model domains at the end of the first model year, 225 days after the last recharge event. This figure is available in colour online at wileyonlinelibrary.com/journal/espl

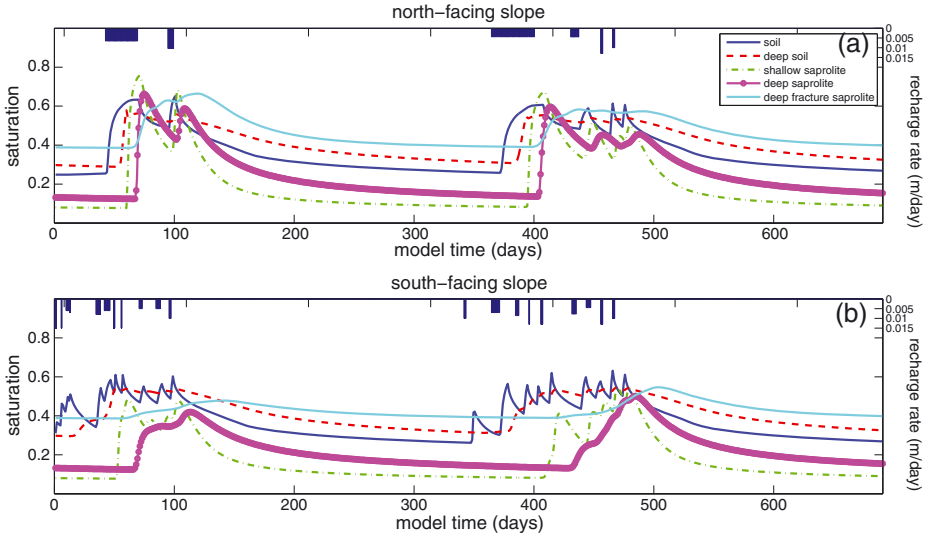

Figure 8. Degree of saturation recorded at five output points in the model domain. Bars at the top of each plot show recharge rate for the two model runs driven by precipitation data from Gordon Gulch. This figure is available in colour online at wileyonlinelibrary.com/journal/espl

m below the soil–saprolite boundary are significantly dried in both models (Figure 7c). In the north-facing slope model, the wetting front reaches the water table and the saprolite is ~ 50% saturated, whereas in the south-facing slope model the

wetting front is ∼0.5 m from the water table and is ∼ 30% saturated. At the end of the model year, after 225 days of evaporation, the soil is dried to the level of residual soil moisture, the only exception being at the base of the hillslopes where the soil intersects with the water table. Where the saprolite is above the water table, it is dried to the value of residual soil moisture in both hillslope models (Figure 7d). Water content at the top of the saprolite is lower than in adjacent soil because of the difference in the *n* parameter, which indicates a wider distribution of pore sizes in the soil (Table I and Figure 6).

Time series of model output at five points in the model domain show how modeled water content varies over the 2-year model runs (Figure 8). Water content in the soil in both models increases to similar levels by the end of the recharge periods. However, water content in the north-facing slope model increases more rapidly and remains elevated for a longer period of time, whereas water content in the south-facing slope model varies more widely and takes longer to reach high levels in response to repeated wetting and drying. In both models, the response to recharge at the deep soil model output point (70 cm below the surface) is damped compared to the response in the shallow soil, and the deep soil dries more slowly than the shallow soil.

The water content at the three model output points in the saprolite varies between the north- and south-facing slope models. On the north-facing slope, water content in the shallow saprolite increases rapidly a few days after the deep soil is wetted (Figure 8a). Ten days after the sharp increase in water content in the shallow saprolite, water content increases rapidly in the deep saprolite, nearly equaling that in the shallow saprolite. The shallow saprolite dries more quickly than the deep saprolite, reaching its residual soil moisture value 100 days after the last recharge pulse, whereas the deep saprolite takes 200 days to dry to residual soil moisture.

On the south-facing slope, the water content in the shallow saprolite increases quickly, but less abruptly than on the north-facing slope (Figure 8b). Twenty days after the large increase in water content at the shallow saprolite model output point, water content in the deep saprolite increases, but less quickly than in the shallow saprolite. As on the north-facing slope, the shallow saprolite dries more quickly than the deep saprolite. The steady-state water content at the model output point near the base of a fracture is higher in both models than at other saprolite model output points because of proximity to the water table (Figure 8). Water content near the base of the corresponding fracture on the north-facing slope increases rapidly and remains elevated for 50 days following the last recharge event before slowly declining to the initial water content. Water content at the comparable south-facing slope site increases modestly and gradually, then declines gradually to the initial water content.

During periods of recharge, when both models showed maximum water content in the saprolite, the degree of saturation on the north-facing slope model is nearly double that of the south-facing slope model (Figure 9). The recharge pulse moves through the saprolite to the water table in both models but, because hydraulic conductivity is higher due to higher water content, the water pulse moves more quickly through the north-facing slope (Figure 9a). In the north-facing slope model, the recharge pulse from the surface reaches the water table ∼15 days following the last recharge event, compared to ∼75 days in the south-facing slope model (Figure 9b).

Water input timing

Data from the north- and south-facing slopes of Gordon Gulch show a clear contrast: north-facing slopes experience prolonged water input from melt of a seasonal snow pack, whereas south-facing slopes experience smaller and more frequent meltwater inputs (Figure 3a). A similar contrast in melt frequency and magnitude occurs along an altitudinal transect as well: higher-altitude sites have seasonal, sustained meltwater pulses (Cowie, 2010). It is of interest, therefore, to consider how differences in the timing of meltwater input, independent of differences in amount, influences subsurface moisture patterns in a mountainous, snow-dominated catchment. To address this issue, we run a set of model calculations in which flow in the model hillslope is driven by recharge input in two different scenarios: a concentrated recharge model in which all recharge occurs during a single prolonged seasonal melt and an episodic recharge model in which the same amount of recharge is distributed among several events. This approach allows us to isolate the role of recharge timing.

The degree of saturation of the model domain during the recharge and drying periods differs significantly between the concentrated recharge model and the episodic recharge model (Figure 10). After all recharge is added to both models (i.e. at the end of the snowmelt season), the wetting front reaches approximately the same depth in the saprolite in both models, but the saprolite in the concentrated recharge model is saturated to ∼ 90% whereas the saprolite in the episodic recharge model is saturated to ∼ 40% (Figure 10a). Ten days following the last recharge event, water begins to drain out of the soil into the saprolite. In the concentrated recharge model, the saprolite near the fractures is drier than the surrounding saprolite at the same depth, because the fractures draw water in from the surrounding matrix (Figure 10b). Twenty-five days after the last recharge (Figure 10c), the top of the saprolite begins to dry in both models. While the wetting front reaches the water table in most of the domain in the concentrated recharge model, the wetting front is still ∼ 1.5 m from the water table in the episodic recharge model. Forty-five days after the last recharge event, the top of saprolite is similarly dry in both models, but the lower saprolite in the concentrated recharge model is still ∼ 50% saturated, and the wetting front in the episodic recharge model has not yet reached the water table (Figure 10d). By the end of the model year, the wetting front has reached the water table in both models and the soil and saprolite are dried to approximately the same extent.

As before, five model output points are placed in the model domain to monitor the degree of saturation throughout the model runs. In the concentrated recharge model run, water content increases immediately following recharge in the shallow soil and increased in the deep soil after a few days of delay (Figure 11a). The shallow saprolite, deep saprolite, and fracture saprolite model output points all show a large, rapid increase in water content early in the model run, before the recharge period ends. Following the recharge period, the soil dries more slowly than the saprolite because water drains from the saprolite relatively quickly, and the deeper locations in both the soil and the saprolite dry more slowly than shallow sites.

In the episodic recharge case, water content in the shallow soil rapidly increases and decays with each precipitation–evaporation cycle (Figure 11b). The wetting and drying response in the deep soil is initially damped and out of phase with the shallow soil response. By day 90 of the model run, the deep soil water content comes into phase with that in the shallow soil. On day 90 of the model run, the wetting front reaches the shallow saprolite and water content increases rapidly. Over the inter-storm evaporation period following day 90, water content in the soil declines little, but moisture declines rapidly in the shallow saprolite. Despite the drying of the shallow saprolite between recharge pulses, water content increases in the shallow saprolite with each recharge pulse following

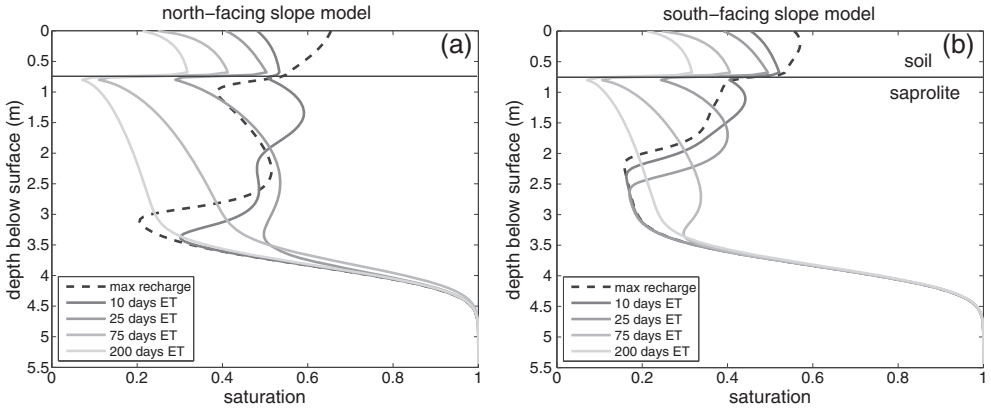

Figure 9. Average degree of saturation for the 3.36 m (84 model cells) closest to the hillslope ridge in the Gordon Gulch models plotted against depth below the surface. (a) North-facing slope. (b) South-facing slope.

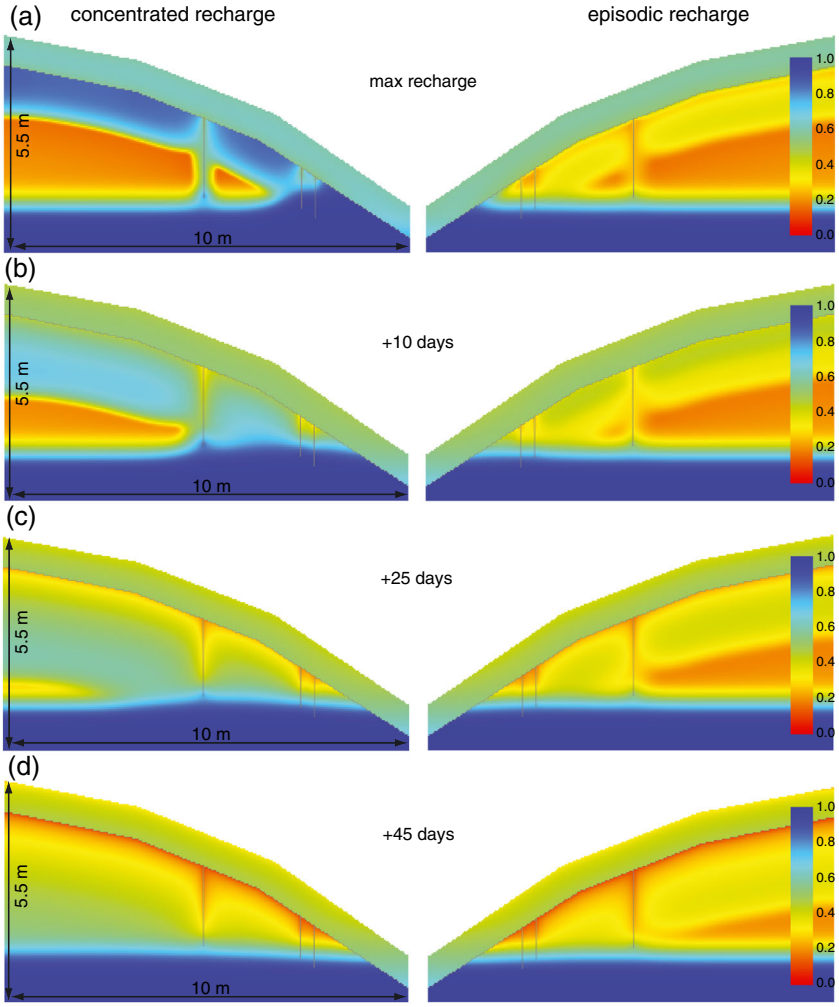

Figure 10. Degree of saturation of the entire model domain for the concentrated and episodic model experiments. The model domains are the same size (5.5 m high, 10 m wide). The water table developed 1 m above the bottom boundary and did not fluctuate significantly during the entire model period. (a) Models on the last day of recharge in the model year. (b) Model domains 10 days after the last recharge event. (c) Model domains 25 days after the last recharge event. (d) Model domains 45 days after the last recharge event. This figure is available in colour online at wileyonlinelibrary.com/journal/espl

day 90 of the model run. The wetting front reaches the deep saprolite after day 115, increases slowly and responds to the remaining recharge events. Water content at the base of the monitored fracture experiences a gradual increase, followed by a gradual decline.

The maximum saturation in the upper 3.5 m of saprolite in the concentrated recharge case is nearly double that of the episodic recharge model (Figure 12). In the concentrated recharge model, the recharge pulse tends to flow quickly through the saprolite as a large pulse with a distinct wetting front, whereas the wetting front in the episodic recharge is more diffuse and moves more slowly. In the concentrated recharge model, the wetting front is 3.5 m below the surface 25 days after the last recharge pulse. Water that is recharged at

the hillcrest of the model, and therefore furthest from the water table in these simulations, reaches the water table at 4.5 m below the surface 30 days after the last recharge (Figure 12a). In the episodic recharge model, the wetting front is 2.5 m below the surface 25 days after the last recharge, and water recharged at the hillcrest does not reach the water table until at least 75 days following the last recharge (Figure 12b).

Discussion

Interaction between soil moisture and water flow in the saprolite

Gordon Gulch is an ideal location to explore the effects of variable recharge input on hillslopes because slope aspect dramatically influences the timing of snow pack melt. Ideally, data would be available from the top of the soil to the water table in order to definitively demonstrate the link between elevated soil moisture in the shallow subsurface and the flow of that water into the deeper subsurface. However, the consistently elevated water content in the soil on the north-facing slope during the spring suggests that any recharge events on the north-facing slope during this period would allow water to flow relatively effectively through the soil and into the underlying saprolite. Higher water content in the unsaturated soil or saprolite allows higher hydraulic conductivity in the medium and faster fluid transport. The wetting and drying on the south-facing slope caused by small, repeated snowmelt events, interspersed with periods of evaporation, result in lower water content and lower effective hydraulic conductivity, which impede water flow deep into subsurface. Soil that dries during periods of evaporation must be re-wetted to some degree with each new precipitation event to allow water to flow, leaving less water to flow into the saprolite.

The soil moisture and matric potential sensors at the Betasso catchment sites were installed directly into the saprolite, unlike the sensors at Gordon Gulch. The magnitude of the precipitation event does not seem to exert primary control on the soil moisture response in the middle and lowest sensors; large precipitation events in the fall of 2010 and early winter of 2011 that caused increased water content at the upper sensor did not produce a response in the lower sensors (Figure 4). The water content and matric potential at the middle and lowest sensors responded only to precipitation events in the spring, after snowmelt had saturated the upper parts of the profile and matric potential remained low at the upper sensor. In April 2011, the addition of new water when matric potential at the

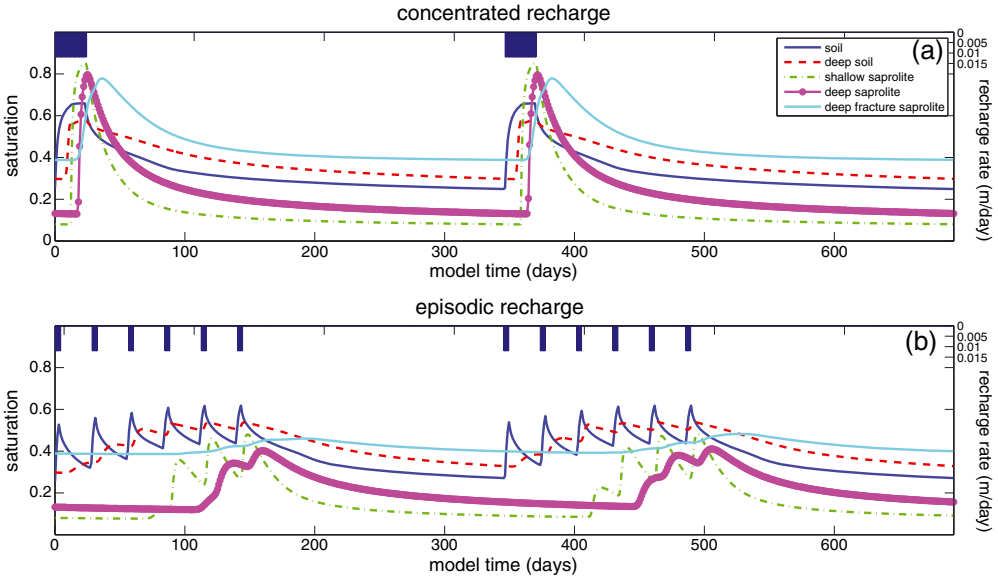

Figure 11. Degree of saturation recorded at five output points in the model domain. Bars at the top of each plot indicate recharge rate for idealized modeling experiments: (a) concentrated recharge; (b) episodic precipitation. This figure is available in colour online at wileyonlinelibrary.com/journal/espl

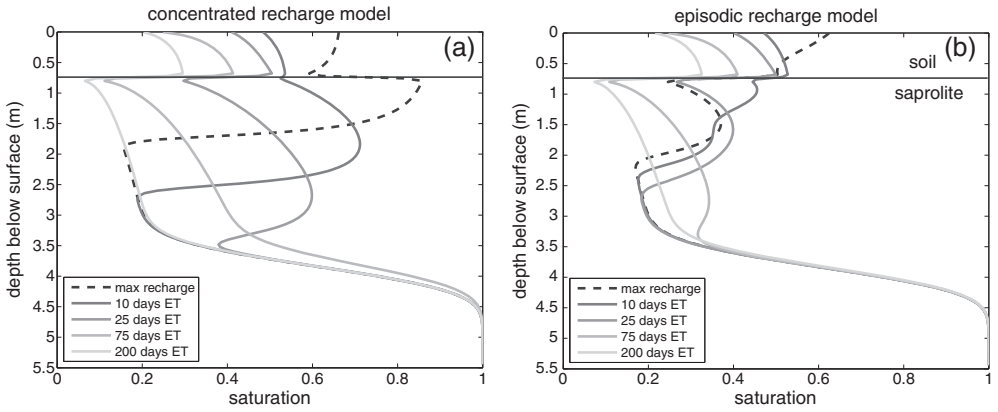

Figure 12. Average degree of saturation for the 3.36 m (84 model cells) closest to the hillslope ridge in the idealized models plotted against depth below the surface: (a) concentrated recharge; (b) episodic recharge. This figure is available in colour online at wileyonlinelibrary.com/journal/espl

upper sensor was low allowed water to flow deeper into the saprolite, both increasing the water content and decreasing the matric potential dramatically at the middle and lowest sensors (Figure 4b,c). Water content at the middle and lowest sensors increased very little following a rain event in late June 2011, although matric potential was low at these locations (Figure 4b,c). Water content was low and matric potential was high at the upper sensor immediately prior to the June 2011 precipitation event. Therefore, the recharged water first had to re-wet the upper part of the profile before flowing deeper into the saprolite, but this recharge event was not large enough to allow flow deeper into the profile. Frequent wetting and drying inhibit fluid flow deep into the subsurface because the soil or saprolite loses moisture to evaporation between precipitation events and must be re-wetted following drying; a large or sustained recharge event is necessary order to drive water into the deep subsurface.

Impact of the timing of recharge

Jones and Banner (2003) show that the distribution of rainfall throughout the year, rather than the average annual precipitation, is the primary control on recharge rates in a tropical karst aquifer. Our results suggest that the timing of melt delivery is also important in mountainous, snow-dominated catchments. Model calculations based on precipitation data from the north- and south-facing slopes of Gordon Gulch imply that the seasonal pattern of snowmelt on a hillslope can exert a significant control on subsurface flow paths, even when the magnitude of total snowmelt over the year is similar. These models indicate that a large sustained recharge pulse, such as the melt of a seasonal snow pack, forces more water deeper into the saprolite matrix and the fractures than repeated, smaller recharge events. The contrast in concentrated recharge and episodic recharge models shows that even when the magnitude of precipitation added to the model, and the number of days of evaporation applied, are the same, the timing of the recharge exerts a surprisingly strong control on the flow paths and degree of saturation in the deep subsurface.

Although the concentrated and episodic recharge models have the same total number of days of evaporation, the episodic recharge model loses 60% more water to evaporation over 2 years than did the concentrated recharge model (47 cm of evaporation vs. 29 cm of evaporation). Evaporation in the episodic recharge model occurs during several intervals when the soil was wet and water can be removed easily, whereas evaporation in the concentrated recharge model begins only after all recharge is applied to the model. Mass balance calculations from the model runs show that recharge that did not leave the model through evaporation flowed out of the base of the model. Fifty-eight centimeters of recharge is applied to both models over the course of each 2-year model run. Thus the concentrated recharge model shows an effective recharge (inflow minus evaporation) to the water table of 29 cm over the 2-year run, whereas the episodic recharge model has an effective recharge of 11 cm over 2 years. Mass balance calculations for the Gordon Gulch models show that the north-facing slope model has an effective recharge of 31 cm over the 2-year model run, whereas the south-facing slope model has an effective recharge of 13 cm. These calculations show that using mean annual precipitation as the sole climate metric for water that flows through the subsurface can be misleading if the timing of the precipitation is not considered. The timing of precipitation exerts a strong control on how deeply into the subsurface water can flow and whether precipitation recharges the deep subsurface at all (Figure 14).

Not surprisingly, fractures in the saprolite allow water to flow more deeply into the subsurface than matrix flow alone. Where fractures are closely spaced, more water flows quickly into the deep subsurface (Figures 7 and 10). In landscapes where fractures are closely spaced, flow in the unsaturated zone may be dominated by fractures rather than the matrix of the saprolite, resulting in faster and deeper flow through the unsaturated zone through these preferential flow paths. In landscapes with large fracture spacing, water will flow uniformly through the saprolite matrix where the saprolite matrix is permeable enough to allow water to flow. A granitic landscape with few initial fractures may not form a permeable saprolite. Water will tend to flow through the soil and along the soil–rock boundary when the recharge rate exceeds the infiltration rate of the rock (Weiler and McDonnell, 2007; Flint *et al.*, 2008). Prolonged contact of water and rock at the soil–rock boundary may form a weathered, more permeable layer in the rock. More flow through fractures may increase dissolution along these flow paths and increase the aperture of the fracture, resulting in a positive feedback between fluid flow and permeability. Increased water flow and potentially more chemical weathering near fractures suggests an intriguing feedback between permeability contrasts that route water in the subsurface and the development of permeability through chemical weathering. On the other hand, precipitation of secondary minerals along preferential flow paths may decrease chemical weathering and permeability by coating minerals along the flow path or blocking the fracture to flow (Megahan and Clayton, 1986).

Model sensitivity

Because there is a large range in published saprolite hydraulic conductivities (Megahan and Clayton, 1986; Katsura *et al.*, 2009), the sensitivity of model results to the selected hydraulic conductivity, K, for saprolite is evaluated by running the concentrated and episodic recharge models with a range of plausible saprolite hydraulic conductivities. The models are run with the saprolite K decreased by a factor of two from the base runs (0.01 m d^{-1}) and increased by a factor of two (0.04 m d^{-1}) and by a factor of four (0.08 m d^{-1}) from the base runs. Decreased saprolite K results in higher saturation at saprolite model output points, higher average saturation with depth, and slower movement of the water pulse through the subsurface. Increased saprolite K results in lower saturation in the models and faster movement of water through the subsurface, with the greatest effects seen in the concentrated recharge models. Mass balance calculations show that effective recharge to the water table in the model runs was not significantly affected by changes to saprolite K.

There are large fluctuations in evapotranspiration rate throughout the year and between the north- and south-facing slopes in Gordon Gulch. The sensitivity of model results to evaporation rate is evaluated by decreasing the evaporation rate by a factor of two and increasing the evaporation rate by a factor of two from the base run (0.0005 and 0.002 m d^{-1}, respectively) for the concentrated and episodic recharge models. Model results for the concentrated recharge model are not sensitive to the evaporation rate. Saturation at model output points and average saturation with depth (Figure 13a, c) do not change significantly when evaporation rate was increased or decreased by a factor of two.

The episodic recharge model is sensitive to changes in evaporation rate (Figure 13b, d). The magnitude of the average saturation with depth increases slightly when evaporation is decreased by half, but the rate at which water flows through the model is greatly increased (Figure 13b). When evaporation is decreased, water reaches the water table ~50 days

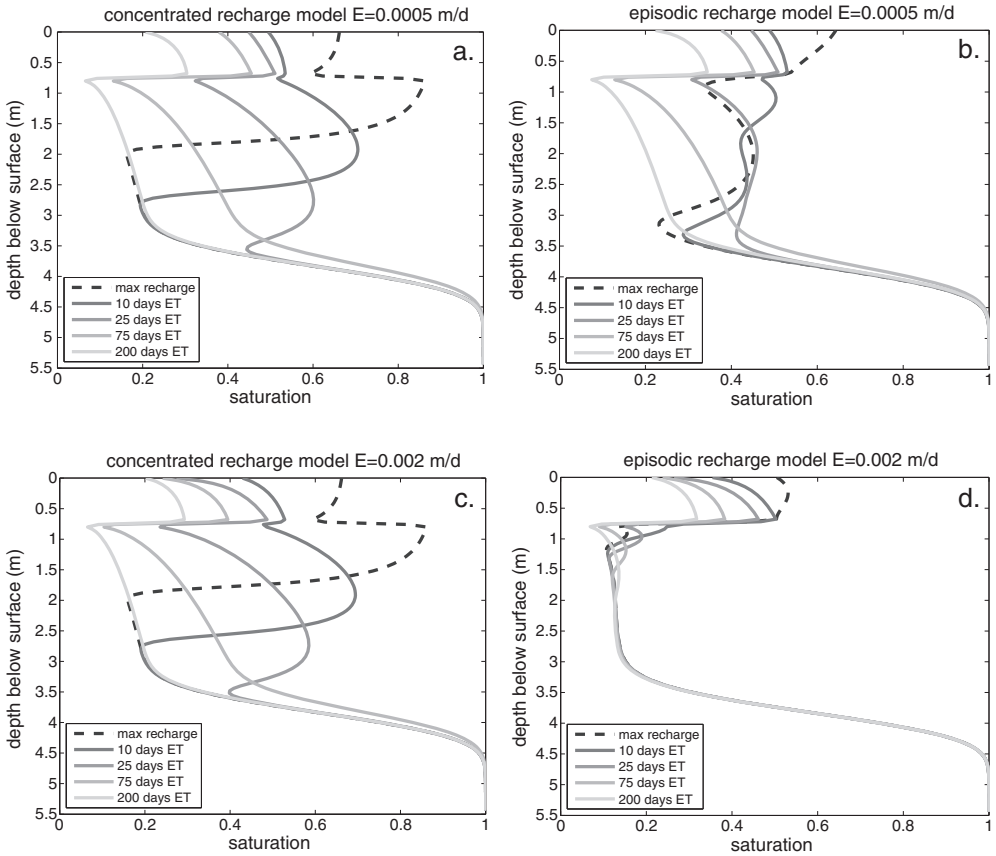

Figure 13. Average degree of saturation with depth below the surface in the model sensitivity runs. (a, b) Evaporation rate was increased by a factor of two for the concentrated and episodic recharge runs, resulting in little change in saturation with depth for the concentrated model run, but a significant increase in saturation and flow velocity for the episodic run. (c, d) Evaporation rate was decreased by a factor of two, resulting in little change in saturation in the concentrated recharge run and significantly decreased saturation and flow velocity in the episodic recharge model.

Table III. Effective recharge to the water table in model sensitivity analysis

Model recharge	Evaporation rate (m d^{-1})	Recharge (cm)
Concentrated	0.0005	34
Episodic	0.0005	27
Concentrated	0.001	28
Episodic	0.001	10
Concentrated	0.002	22
Episodic	0.002	−6

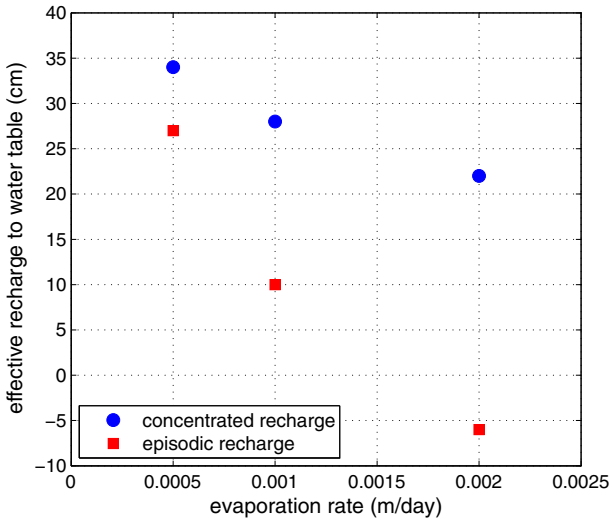

Figure 14. Effective recharge to water table in concentrated recharge and episodic recharge model runs plotted against daily evaporation rate. As evaporation rate increases, effective recharge to the decreases for both model runs and the effect of a concentrated recharge pulse on flow in the deep unsaturated zone becomes more pronounced. This figure is available in colour online at wileyonlinelibrary.com/journal/espl

faster than in the base model. Mass balance calculations show that, when the evaporation rate is decreased by half, effective recharge to the water table over two model years nearly triples from 10 cm to 27 cm (Table III and Figure 14). When the evaporation rate is increased by a factor of two, water flow through the saprolite becomes almost non-existent (Figure 13d). With a high evaporation rate, effective recharge to the water table becomes negative, with more water leaving the model over 2 years than is added over the same time (Table III and Figure 14).

Where evaporation rates are low, the importance of the episodicity of water influx to flow in the deep subsurface begins to decline and model results from concentrated recharge models and episodic recharge models become more similar (Figure 14). However, evaporation rates on south-facing hillslopes are likely to be higher than on north-facing hillslopes due to higher temperature, higher radiation and, in many mountain catchments in the western USA, less shade. When evaporation rates are high, episodicity of water influx becomes much more important to flow in the deep subsurface. When the evaporation rate is high, a concentrated recharge pulse allows water to flow quickly into the deep subsurface and to be sequestered from the high

evaporation rate at the surface. Episodic recharge pulses saturate the top of the profile, but that water is quickly removed by high evaporation before it can flow into the deep subsurface.

Implications for chemical weathering and climate change

Larger water fluxes through model hillslopes after a large, sustained recharge pulse may help explain differences in soil depth and weathering intensity between the north- and south-facing slopes observed at Gordon Gulch. The north-facing slope has deeper soil, more weathered saprolite, and greater depth to fresh rock compared to the south-facing slope (Befus *et al.*, 2011; Anderson *et al.*, 2011; Kelly, 2012). Sustained elevated water content on hillslopes following a concentrated recharge pulse suggests that more chemical weathering may occur on hillslopes with a seasonal snow pack compared to hillslopes with intermittent snow. The melt of a seasonal snow pack allows water to flow faster and more deeply into the subsurface, where the transformation of rock into saprolite can occur. Water delivered to the soil or saprolite after a short recharge event moves more slowly through the subsurface, resulting in slower chemical weathering rates and a more shallow weathering front (Maher, 2010).

Geochemical modeling (Lebedeva *et al.*, 2010) shows that the thickness of weathered material increases with pore fluid velocity, which is assumed to be proportional to mean annual precipitation. In recent studies, low chemical weathering rates have been attributed to lack of water in the subsurface (Dixon *et al.*, 2009; Ferrier *et al.*, 2012). Our model results suggest that chemical weathering rates are strongly controlled not just by the mean annual precipitation but also by the duration over which this precipitation enters the subsurface. This finding is important for snow-dominated mountain catchments, and may imply a transition in behavior as the seasonal snow pack becomes more marginal.

The results of this study have implications for how the rate and primary areas of bedrock weathering may change with a changing climate, and how rates and distributions of chemical weathering may have been different in the past. In the western USA, snowmelt contributes a disproportionately larger amount to groundwater recharge than average annual precipitation would predict (Simpson *et al.*, 1970; Winograd *et al.*, 1998). A warming global climate is expected to increase the amount of precipitation that falls as rain, and to accelerate snow pack melting both in the Colorado Rockies (Rasmussen *et al.*, 2011) and throughout the Northern Hemisphere (Schlaepfer *et al.*, 2012). Climate change that results in decreased snow pack, even with constant annual precipitation, is predicted to result in decreased groundwater recharge (Earman *et al.*, 2006). Our model calculations suggest that reducing the area that is covered by a seasonal snow pack will result in reduced water flux to and through the deep unsaturated zone. This will therefore reduce chemical weathering rates in the saprolite and diminish groundwater recharge in small mountain catchments. Conversely, increasing the area covered by a seasonal snow pack on a mountain landscape would result in more area with larger water fluxes through hillslopes.

Conclusions

The episodicity of recharge, independent of magnitude, can strongly influence water fluxes in the subsurface of mountain hillslopes. Data collected in the Boulder Creek watershed demonstrate that in locations with a seasonal snow pack (e.g. pole-facing hillslopes), soil moisture increases following the spring snowmelt and remains elevated for several months. In locations with intermittent snowmelt events (e.g. Equator-facing hillslopes), soil moisture is more variable through time and water can only flow into the deeper subsurface on rare occasions when the shallow soil is sufficiently saturated.

Model calculations imply that the primary control on the speed and extent of water flow below the surface is the episodicity of the recharge. In a model scenario driven by a prolonged period of recharge, meant to mimic the melt of a seasonal snow pack, more water moves deeply through the hillslope and recharges the water table. In a model scenario with the same magnitude of recharge spread out over several shorter-duration events, water moves through the hillslope more slowly and recharge to the water table is reduced by more than 50%. These findings have implications for both chemical weathering and water chemistry in the subsurface and changes in groundwater recharge in the past as well as the future.

Recent studies have found that water supply is of critical importance to chemical weathering rates in soils and saprolite (Dixon *et al.*, 2009; Maher, 2010; Rasmussen *et al.*, 2011; Ferrier *et al.*, 2012). Our results suggest that locations with a seasonal snow pack may experience more chemical weathering in the subsurface than locations with the same amount of snow melt spread over several events. Our results highlight a potential pitfall in using mean annual precipitation as the sole climate metric for evaluating the relationship between chemical weathering and climate. Mean annual precipitation alone is not a faithful proxy of how much water fluxes to the weathering front if the episodicity of the precipitation is not considered.

Acknowledgments—This work was funded by NSF grant EAR-0724960 to SPA. We thank the faculty, staff, and students associated with the Boulder Creek Critical Zone Observatory for their assistance on this project, especially Nathan Rock and Eve-Lyn Hinckley.

References

Anderson RS, Anderson SP, Tucker GE. 2013. Rock damage and regolith transport by frost: an example of climate modulation of the geomorphology of the critical zone. *Earth Surface Processes and Landforms* **38**: 299–316.

Anderson S, von Blanckenburg F, White A. 2007. Physical and chemical controls on the critical zone. *Elements* **3**(5): 315–319.

Anderson SP, Dietrich WE, Montgomery DR, Torres R, Conrad ME, Loague K. 1997. Subsurface flow paths in a steep, unchanneled catchment. *Water Resources Research* **33**(12): 2637–2653.

Anderson SP, Dietrich WE, Brimhall GH. 2002. Weathering profiles, mass-balance analysis, and rates of solute loss: linkages between weathering and erosion in a small, steep catchment. *Geological Society of America Bulletin* **114**(9): 1143–1158.

Anderson SP, Anderson RS, Hinckley E, Kelly P, Blum A. 2011. Exploring weathering and regolith transport controls on critical zone development with models and natural experiments. *Applied Geochemistry* **26**: S3–S5.

Befus K, Sheehan A, Leopold M, Anderson S, Anderson R. 2011. Seismic constraints on critical zone architecture, Boulder Creek watershed, Front Range, Colorado. *Vadose Zone Journal* **10**(3): 915–927.

Berkowitz B. 2002. Characterizing flow and transport in fractured geological media: a review. *Advances in Water Resources* **25**(8): 861–884.

Beven K, Germann P. 2013. Macropores and water flow in soils revisited. *Water Resources Research* **49**: 3071–3092.

Brantley SL, Lebedeva M. 2011. Learning to read the chemistry of regolith to understand the critical zone. *Annual Review of Earth and Planetary Sciences* **39**: 387–416.

Brantley SL, White AF. 2009. Approaches to modeling weathered regolith. *Reviews in Mineralogy and Geochemistry* **70**(1): 435–484.

Cowie R. 2010. *The hydrology of headwater catchments from the plains to the continental divide, Boulder Creek watershed, Colorado*. Master's thesis, University of Colorado.

Dengler EL. 2010. *Fracture distribution and characterization in Betasso Gulch, CO*. Master's thesis, Bates College.

Dixon JL, Heimsath AM, Amundson R. 2009. The critical role of climate and saprolite weathering in landscape evolution. *Earth Surface Processes and Landforms* **34**(11): 1507–1521.

Earman S, Campbell AR, Phillips FM, Newman BD. 2006. Isotopic exchange between snow and atmospheric water vapor: estimation of the snowmelt component of groundwater recharge in the southwestern united states. *Journal of Geophysical Research: Atmospheres* **111**(D9). DOI: 10.1029/2005JD006,470.

Ebel BA, Loague K, Vanderkwaak JE, Dietrich WE, Montgomery DR, Torres R, Anderson SP. 2007. Near-surface hydrologic response for a steep, unchanneled catchment near Coos Bay, Oregon. 2. Physics-based simulations. *American Journal of Science* **307**(4): 709–748.

Egli M, Mirabella A, Sartori G, Zanelli R, Bischof S. 2006. Effect of north and south exposure on weathering rates and clay mineral formation in Alpine soils. *Catena* **67**(3): 155–174.

Ferrier KL, Kirchner JW, Finkel RC. 2012. Weak influences of climate and mineral supply rates on chemical erosion rates: measurements along two altitudinal transects in the Idaho Batholith. *Journal of Geophysical Research* **117**(F2). DOI: 10.1029/2011JF002,231.

Flint AL, Flint LE, Dettinger MD. 2008. Modeling soil moisture processes and recharge under a melting snowpack. *Vadose Zone Journal* **7**(1): 350–357.

Glass RJ, Nicholl MJ, Tidwell VC. 1995. Challenging models for flow in unsaturated, fractured rock through exploration of small scale processes. *Geophysical Research Letters* **22**(11): 1457–1460.

Graham CB, Van Verseveld W, Barnard HR, McDonnell JJ. 2010. Estimating the deep seepage component of the hillslope and catchment water balance within a measurement uncertainty framework. *Hydrological Processes* **24**(25): 3631–3647.

Healy RW. 2008. Simulating water, solute, and heat transport in the subsurface with the VS2DI software package. *Vadose Zone Journal* **7**(2): 632–639.

Hinckley ES, Ebel BA, Barnes RT, Anderson RS, Williams MW, Anderson SP. 2014. Aspect control of water movement on hillslopes near the rain-snow transition of the Colorado Front Range. *Hydrological Processes* **28**(1): 74–85.

Hopp L, McDonnell JJ. 2009. Connectivity at the hillslope scale: identifying interactions between storm size, bedrock permeability, slope angle and soil depth. *Journal of Hydrology* **376**(3): 378–391.

Jenny H. 1941. *Factors of Soil Formation*. McGraw-Hill: New York.

Jones IC, Banner JL. 2003. Hydrogeologic and climatic influences on spatial and interannual variation of recharge to a tropical karst island aquifer. *Water Resources Research* **39**(9): 5-1–5-10.

Katsura S, Kosugi K, Mizutani T, Mizuyama T. 2009. Hydraulic properties of variously weathered granitic bedrock in headwater catchments. *Vadose Zone Journal* **8**(3): 557–573.

Kelly PJ. 2012. *Subsurface evolution: characterizing the physical and geochemical changes in weathered bedrock of lower Gordon Gulch, Boulder Creek Critical Zone Observatory*. Master's thesis, University of Colorado.

Kosugi K, Katsura S, Katsuyama M, Mizuyama T. 2006. Water flow processes in weathered granitic bedrock and their effects on runoff generation in a small headwater catchment. *Water Resources Research* **42**(2). DOI: 10.1029/2005WR004275.

Lappala EG, Healy RW, Weeks EP. 1987. Documentation of computer program VS2D to solve the equations of fluid flow in variably saturated porous media, *US Geological Survey Water Resources Investigations Report 83-4099*.

Lebedeva MI, Fletcher RC, Balashov VN, Brantley SL. 2007. A reactive diffusion model describing transformation of bedrock to saprolite. *Chemical Geology* **244**(3–4): 624–645.

Lebedeva MI, Fletcher RC, Brantley SL. 2010. A mathematical model for steady-state regolith production at constant erosion rate. *Earth Surface Processes and Landforms* **35**(5): 508–524.

Maher K. 2010. The dependence of chemical weathering rates on fluid residence time. *Earth and Planetary Science Letters* **294**(1): 101–110.

Megahan WF, Clayton JL. 1986. Saturated hydraulic conductivities of granitic materials of the Idaho Batholith. *Journal of Hydrology* **84**(1–2): 167–180.

Montgomery DR, Dietrich WE, Torres R, Prestrud Anderson S, Heffner JT, Loague K. 1997. Hydrologic response of a steep, unchanneled valley to natural and applied rainfall. *Water Resources Research* **33**(1): 91–109.

Rasmussen C, Brantley SL, Richter D, Blum AE, Dixon JL, White AF. 2011. Strong climate and tectonic control on plagioclase weathering in granitic terrain. *Earth and Planetary Science Letters* **301**(3): 521–530.

Rasmussen R, Liu C, Ikeda K, Gochis D, Yates D, Chen F, Tewari M, Barlage M, Dudhia J, Yu W, Miller K, Arsenault K, Grubisic V, Thompson G, Gutmann E. 2011. High-resolution coupled climate runoff simulations of seasonal snowfall over Colorado: a process study of current and warmer climate. *Journal of Climate* **24**(12): 3015–3048.

Riebe CS, Kirchner JW, Finkel RC. 2004. Erosional and climatic effects on long-term chemical weathering rates in granitic landscapes spanning diverse climate regimes. *Earth and Planetary Science Letters* **224**(3–4): 547–562.

Sacks WJ, Schimel DS, Monson RK, Braswell BH. 2006. Model-data synthesis of diurnal and seasonal CO_2 fluxes at Niwot Ridge, Colorado. *Global Change Biology* **12**(2): 240–259.

Schlaepfer DR, Lauenroth WK, Bradford JB. 2012. Consequences of declining snow accumulation for water balance of mid-latitude dry regions. *Global Change Biology* **18**: 1988–1997.

Simpson ES, Thorud DB, Friedman I. 1970. Distinguishing seasonal recharge to groundwater by deuterium analysis in southern Arizona. *International Association of Hydrology Publication* **92**: 112–121.

van Genuchten MT. 1980. A closed-form equation for predicting the hydraulic conductivity of unsaturated soils. *Soil Science Society of America Journal* **44**(5): 892–898.

Weiler M, McDonnell JJ. 2007. Conceptualizing lateral preferential flow and flow networks and simulating the effects on gauged and ungauged hillslopes. *Water Resources Research* **43**(3). DOI: 10.1029/2006WR004867.

Western Regional Climate Center. 2012. Average pan evaporation data by state. Available: http://www.wrcc.dri.edu/climatedata/tables/ [18 February 2015].

White AF, Blum AE. 1995. Effects of climate on chemical weathering in watersheds. *Geochimica et Cosmochimica Acta* **59**(9): 1729–1747.

White AF, Blum AE, Schulz MS, Vivit DV, Stonestrom DA, Larsen M, Murphy SF, Eberl D. 1998. Chemical weathering in a tropical watershed, Luquillo Mountains, Puerto Rico. I. Long-term versus short-term weathering fluxes. *Geochimica et Cosmochimica Acta* **62**(2): 209–226.

Williams CJ, McNamara JP, Chandler DG. 2008. Controls on the temporal and spatial variability of soil moisture in a mountainous landscape: the signatures of snow and complex terrain. *Hydrology and Earth System Sciences* **5**: 1927–1966.

Winograd IJ, Riggs AC, Coplen TB. 1998. The relative contributions of summer and cool-season precipitation to groundwater recharge, Spring Mountains, Nevada, USA. *Hydrogeology Journal* **6**(1): 77–93.

Woods R, Rowe L. 1996. The changing spatial variability of subsurface flow across a hillside. *Journal of Hydrology (NZ)* **35**(1): 51–86.